THE JOURNAL OF PHYSICAL CHEMISTRY A LETTERS

2008, *112,* 4863–4868
Published on Web 05/08/2008

Residue-Based Charge Flipping: A New Variant of an Emerging Algorithm for Structure Solution from X-ray Diffraction Data

Zhongfu Zhou and Kenneth D. M. Harris*

School of Chemistry, Cardiff University, Park Place, Cardiff CF10 3AT, Wales

Received: February 8, 2008

There is currently substantial interest and activity in the development and application of a new technique, called "charge flipping" (CF), that has emerged in the past few years for carrying out structure solution from X-ray diffraction data. We report here a new variant of this technique, termed "residue-based charge flipping" (RBCF), in which the residues of calculated and experimental structure factor amplitudes, together with the corresponding electron density residues, are introduced within the CF algorithm. An important feature of this approach is that it does not require a positive threshold electron density value (δ) to be specified to control the charge-flipping step within the algorithm (in contrast, it is well established that the success of standard CF calculations can depend critically on choosing a suitable value of δ for a given structural problem). Methodological details of the RBCF algorithm are described, and the results of the application of this technique for structure solution of three test structures are reported. The RBCF technique is shown to lead to the correct structure solution in all cases, with success rates of at least 90% (for independent calculations from different sets of initial random phases). Significantly, the convergence behavior of RBCF calculations is found to contrast markedly with that generally observed for standard CF calculations. In particular, convergence (assessed from the evolution of *R*-factor versus iteration number) typically progresses rapidly and immediately from the earliest iterations of RBCF calculations, rather than displaying an extended plateau region. This feature, and the fact that the RBCF technique does not use the δ parameter that is required in standard CF calculations, suggest that the RBCF algorithm may be a promising approach in future applications.

1. Introduction

Structure determination of crystalline solids using X-ray diffraction data is well established as a powerful tool in structural science. Indeed, X-ray diffraction techniques have made a significant impact in advancing a broad range of scientific fields, both fundamental and applied, given that many phenomena in the physical, chemical, materials and biological sciences can be understood directly from knowledge of crystal structures.

X-ray diffraction experiments are commonly carried out on single-crystal specimens or powder (polycrystalline) samples, and although the underlying phenomenon is the same, the different form of the diffraction data obtained in single-crystal and powder diffraction experiments is such that aspects of the data analysis are different in each case. For both single-crystal and powder X-ray diffraction data, however, very powerful techniques have been developed to allow crystal structure determination to be carried out, particularly with regard to tackling the challenge of overcoming the "phase problem" during the structure solution stage of the structure determination process. Thus, the development of techniques such as direct methods and Patterson methods represented revolutionary advances in crystal structure determination,[1] both for single-crystal and powder X-ray diffraction data. Also, recently developed strategies for direct-space structure solution have advanced the opportunities for carrying out complete structure determination from powder X-ray diffraction data in the case of molecular materials.[2] Although the techniques discussed above for carrying out structure solution from single-crystal and powder X-ray diffraction data are now well established, there nevertheless remains scope for the development and exploration of new and alternative methodologies that may have the potential to provide advantages in certain areas of application.

In this regard, there is significant current interest in a new technique, termed "charge flipping" (CF), that has emerged in the past few years for carrying out structure solution from X-ray diffraction data, following the first work on this technique published by Oszlányi and Sütő in 2004.[3,4] This new (and amazingly simple) computational algorithm has been shown to have considerable potential in a range of challenging situations encountered in structure determination, including difficult cases of structure solution,[5] structure solution from incomplete data,[6] cases of pseudosymmetry,[7] and structure solution of incommensurate structures[8–10] and quasicrystals.[11] The technique has also been adapted successfully for structure solution from powder X-ray diffraction data,[12,13] and an implementation suitable for neutron diffraction data has also been reported.[14] Although the development of the CF technique has made rapid progress and the technique shows considerable promise, it is nevertheless relevant to note that its application is associated with some inherent drawbacks that are not yet fully resolved, and these issues are elaborated in more detail in Section 2 below.

With a view to assessing some of these issues, we have recently focused on exploring new implementations of the CF concept, and in the present paper we report a new variant of

* Author for correspondence. E-mail: HarrisKDM@cardiff.ac.uk.

10.1021/jp801185u CCC: $40.75

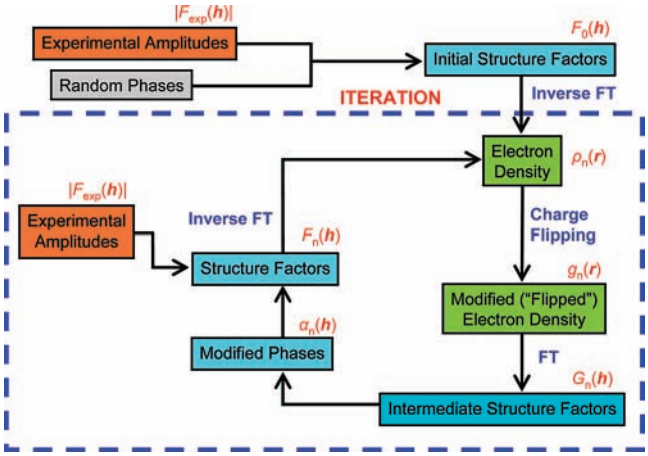

Figure 1. Schematic flow-chart of the standard CF algorithm.

the CF strategy, which we call "residue-based charge flipping" (RBCF). In principle, the RBCF algorithm should be equally applicable to both single-crystal and powder X-ray diffraction data, although in the present paper we specifically demonstrate the application of the technique in the case of structure solution from single-crystal X-ray diffraction data.

2. Resumé of the Standard Charge Flipping Algorithm

Before highlighting specific details of the RBCF technique, it is relevant first to give a resumé of the standard CF algorithm. A simplified flow-chart of the standard CF algorithm is shown in Figure 1. Initially, the calculation starts from the experimentally determined structure factor amplitudes $F_{exp}(h)$ for all reflections h (e.g., obtained from measured X-ray diffraction intensities) together with randomly generated phases for each reflection h, to generate the initial set of structure factors $F_0(h)$ (throughout this paper, subscripts n refer to the iteration number within the CF calculation). The electron density $\rho_1(r)$ (for iteration $n = 1$) is then calculated from the set of structure factors $F_0(h)$ by the inverse Fourier transform. The electron density $\rho_1(r)$ is then subjected to the charge flipping step, in which a modified ("flipped") electron density $g_1(r)$ is generated by reversing the sign of any electron density for which $\rho_1(r) < \delta$ (note: $\delta \geq 0$), where δ is a positive user-specified threshold parameter. Thus,

$$\begin{aligned} &\text{if } \rho_1(r) \geq \delta, \text{ then } g_1(r) = \rho_1(r) \\ &\text{if } \rho_1(r) < \delta, \text{ then } g_1(r) = -\rho_1(r) \end{aligned} \quad (1)$$

We emphasize that the flipping procedure is such that all negative values of $\rho_1(r)$ are flipped to become positive, whereas all small positive values of $\rho_1(r)$ [i.e., within the range $0 < \rho_1(r) < \delta$] are flipped to become negative. The importance of including some amount of negative electron density has been elaborated elsewhere.[3,15]

A set of intermediate structure factors $G_1(h)$ are then generated from the Fourier transform of $g_1(r)$, but only the phases $\alpha_1(h)$ of these structure factors are actually used. Thus, the set of phases $\alpha_1(h)$ are taken together with the experimental structure factor amplitudes $F_{exp}(h)$ to generate the updated structure factors $F_1(h)$ [note that in the standard CF algorithm, the amplitudes of the intermediate structure factors $|G_n(h)|$ are never actually used in the calculation, except in determination of the R-factor, which is used solely to monitor progress of the calculation].

The next iterative cycle ($n = 2$) starts by calculating a new electron density $\rho_2(r)$ from the inverse Fourier transform of $F_1(h)$, and the iterative procedure is then repeated. Each iteration n starts from the set of structure factors $F_{n-1}(h)$ obtained in the previous iteration and proceeds to generate $\rho_n(r)$, $g_n(r)$, $G_n(h)$ and finally the updated structure factors $F_n(h)$. An important consideration is the way in which the structure factor $F_n(0)$ (corresponding to the total number of electrons in the unit cell) is handled during the CF calculation, and two approaches have been used in the previously published work: (i) $F_n(0)$ is allowed to vary during the calculation,[3] or (ii) $F_n(0)$ is fixed at $F_n(0) = 0$ throughout the calculation.[8,16] Consequences of these different approaches are discussed in the references cited (as discussed in section 3, our implementation of the RBCF technique adopts approach (ii)).

The calculation is carried out until the R-factor converges upon an acceptable value and the structure solution $\rho_n(r)$ obtained is of adequate quality to be used as a starting point for structure refinement. We emphasize that the R-factor does not in any way drive the iterative process but is used simply to monitor progress of the calculation. As elaborated previously,[3,4] CF calculations are generally carried out in space group $P1$, and hence an assignment of the space group may be established by inspection of symmetry within the unit cell in the structure solution (i.e., the final electron density map) obtained from the CF calculation.

Although considerable advances have been made in the application of the CF technique since its recent inception, it is important to draw attention to certain features of the technique.[3,15–17] First, the standard CF algorithm requires a threshold parameter δ to be specified to control the charge flipping step, but it is found that the correct selection of this parameter is often critical for the successful application of the technique. There is currently no analytical approach for determining a priori the optimal value of δ to be used for any specific structural problem,[17] and moreover, the optimal value of δ appears to be problem-specific. Although empirical approaches for estimating δ have been proposed,[4,17] the fact that the success of the calculations is sensitive to the optimal choice of this parameter remains a troublesome feature of the technique. Furthermore, the success rate of the standard CF technique can be low in the case of difficult structures,[4,16] partly because success depends heavily on the value of δ.[17] Second, a commonly observed feature of standard CF calculations is that the iterative process generally displays a significant period of "stagnation" (corresponding to a high value of R-factor that does not change substantially over a large number of iterations) before convergence on a correct solution with low R-factor is finally achieved. This "stagnant" period of the calculation can extend over a substantial number of iterations in the case of difficult structures.[16] Thus, the evolution of R-factor as a function of iteration number generally shows a long plateau region in which R-factor remains relatively constant at a high value over a large number of iterations, before dropping rapidly as convergence occurs on the correct structure solution. There are many illustrations of this behavior in the existing literature on applications of the standard CF technique [for typical examples of such plots of R-factor versus iteration number; see Figure 2 (middle) of ref 3, Figure 2 of ref 10 or Figure 1 of ref 16].

3. Methodology of Residue-Based Charge Flipping

A flow-chart of the RBCF algorithm is shown in Figure 2 (and should be compared to the corresponding flow-chart for the standard CF algorithm in Figure 1). As mentioned in section

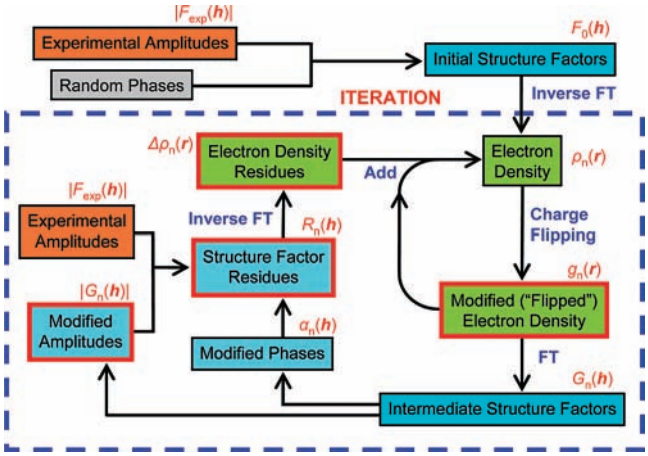

Figure 2. Schematic flow-chart of the new RBCF algorithm.

2, our RBCF algorithm follows the approach of fixing $F_n(0)$ at $F_n(0) = 0$ throughout the calculation, as adopted in several implementations of standard CF, with the consequence that the electron densities discussed below are expressed relative to the average electron density in the unit cell.

RBCF differs from standard CF in two crucial ways highlighted in Figure 2 (the parts that differ from the standard CF algorithm are highlighted in red boxes). First, after calculating the intermediate structure factors $G_n(h)$ from the modified ("flipped") electron density $g_n(r)$ (in iteration n), we do *not* then combine the phases $\alpha_n(h)$ [from $G_n(h)$] with the experimental structure factor amplitudes $|F_{exp}(h)|$ to generate new structure factors $F_n(h)$. Instead, the phases $\alpha_n(h)$ of the intermediate structure factors $G_n(h)$ are combined with the *difference* between the intermediate structure factor amplitudes $|G_n(h)|$ and the experimental structure factor amplitudes $|F_{exp}(h)|$. The resultant *structure factor residues*, denoted $R_n(h)$, are thus given by

$$R_n(h) = [|F_{exp}(h)| - |G_n(h)|] \times [G_n(h)/|G_n(h)|] \quad (2)$$

where $[|F_{exp}(h)| - |G_n(h)|]$ is the difference in structure factor amplitudes and $[G_n(h)/|G_n(h)|]$ is the phase part of $G_n(h)$. The structure factor residues are then used to calculate (by inverse Fourier transform) the corresponding electron density residues $\Delta\rho_n(r)$:

$$\Delta\rho_n(r) = (1/V)\sum_h \{R_n(h) \exp(-2\pi i h \cdot r)\} \quad (3)$$

where V is the volume of the unit cell. The new electron density $\rho_{n+1}(r)$ is then obtained from

$$\rho_{n+1}(r) = \Delta\rho_n(r) + g_n(r) \quad (4)$$

where $g_n(r)$ is the modified electron density obtained earlier in the same iteration following the charge flipping step. The new electron density $\rho_{n+1}(r)$ is then used to start the next iterative cycle.

The second crucial difference with respect to the standard CF algorithm concerns the way in which the actual charge flipping step is carried out. Thus, in contrast to eq 1, charge flipping of the electron density $\rho_n(r)$ to generate the "flipped" electron density $g_n'(r)$ is carried out simply by reversing the sign of any negative electron density:

$$\text{if } \rho_n(r) \geq 0, \text{ then } g_n'(r) = \rho_n(r)$$
$$\text{if } \rho_n(r) < 0, \text{ then } g_n'(r) = -\rho_n(r) \quad (5)$$

Clearly, the flipped electron density $g_n'(r)$ is positive everywhere. However, the fact that we adopt the approach of fixing $F_n(0) = 0$ throughout the calculation requires that the electron density should have an average value of zero. Thus, the "flipped" electron density $g_n'(r)$ is adjusted as follows:

$$g_n(r) = g_n'(r) - \langle g_n'(r) \rangle \quad (6)$$

to produce the modified "flipped" electron density $g_n(r)$, where $\langle g_n'(r) \rangle$ denotes the value of $g_n'(r)$ averaged over the whole unit cell. The electron density $g_n(r)$ is then used to calculate the intermediate structure factors $G_n(h)$ by Fourier transformation.

It is important to note that, in eq 5, the charge flipping step does not involve any user-specified threshold parameter δ (or, alternatively, can be regarded as equivalent to the procedure used in the standard CF algorithm for the case with $\delta = 0$). In this regard, RBCF can be considered as a genuinely ab initio technique, as the application of the technique does not rely on the appropriate choice of any control parameter. This contrast between the standard CF and RBCF algorithms originates from features of the inverse Fourier transform, which is used (see Figures 1 and 2) to convert from structure factors to electron density in standard CF, or to convert from structure factor residues to electron density residues in RBCF. If (as in both standard CF and RBCF) the inverse Fourier transform is applied to a finite domain of data (i.e., a finite number of structure factors or structure factor residues), oscillations are introduced into the resultant map of electron density or electron density residues. As discussed elsewhere,[3,4,15] the δ parameter in the standard CF algorithm can be regarded as serving the role of covering the range of these oscillations. However, there is a major difference between standard CF and RBCF in terms of the *amplitudes* of the input data for the inverse Fourier transform, and in particular the way in which these amplitudes vary as the calculation progresses. Thus, throughout the standard CF calculation (i.e., for all iteration numbers n), the inverse Fourier transform is carried out on a domain of constant "size" and "magnitude" (i.e., a finite number of structure factors with amplitudes given by the experimental data). In the RBCF calculation, on the other hand, the inverse Fourier transform is carried out on the structure factor residues, and thus although the domain on which the inverse Fourier transform is applied remains constant in "size" (i.e., a finite number of structure factor residues), the "magnitude" of this domain (i.e., the amplitudes of the structure factor residues) should generally decrease as the calculation progresses (although small oscillations may still be exhibited as the calculation converges close to the correct structure solution). Thus, as the RBCF calculation proceeds through successive iterations and the quality of the structure solution improves, the amplitudes of the structure factor residues will decrease, ultimately approaching very small values. As a consequence, the oscillations introduced into the electron density residue map due to finite-size effects of the inverse Fourier transform should also diminish during the calculation, as the RBCF calculation progresses to successful convergence. Thus, as demonstrated below, no adverse effects are encountered simply by setting the threshold parameter δ to zero in the RBCF calculation (even in the early iterations).

4. Results and Discussion

We now discuss our preliminary studies to test the RBCF technique using single-crystal X-ray diffraction data for three known crystal structures: (1) *N*,*N*′-(2,5-diamino-2,5-cyclohexadiene-1,4-diylidene)bis(1,4-benzenediamine) (denoted **1**; Scheme 1),[18] (2) the zeolite ferrierite in the purely siliceous form (denoted **2**),[19] and (3) hexabromobenzene (denoted **3**; Scheme 1).[20,21] For structure **1**, experimental single-crystal X-ray dif-

SCHEME 1: Molecular Structures of 1 and 3

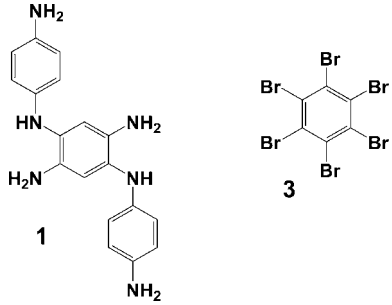

TABLE 1: Relevant Crystallographic Data for Test Structures 1 − 3[a]

	structure **1**	structure **2**	structure **3**
asymmetric unit	$C_{18}H_{20}N_6$	Si_4O_8	C_6Br_6
Z	4	16	4
space group	$P2_1/n$	$Immm$	$P2_1/n$
a/Å	5.355	19.018	8.326
b/Å	7.910	14.303	3.949
c/Å	18.243	7.541	15.271
β/deg	93.24	-	92.93
h range	−4 → +4	−18 → +18	−7 → +7
k range	−6 → +6	−14 → +14	−3 → +3
l range	0 → +14	0 → +7	0 → +14
Δx/Å	0.18 Å	0.24 Å	0.21 Å
Δy/Å	0.20 Å	0.29 Å	0.20 Å
Δz/Å	0.20 Å	0.25 Å	0.25 Å
direct-space resolution	1.2 Å	1.0 Å	1.0 Å

[a] The dimensions of the voxels in the unit cell, used in the calculation of electron density in the RBCF calculation, are denoted Δx, Δy and Δz. The direct-space resolution is determined from the maximum 2θ angle in the diffraction data.

fraction data were used,[22] whereas for structures **2** and **3**, simulated single-crystal X-ray diffraction data were used, with structure factor amplitudes calculated from the published crystal structures. Relevant crystallographic information for each of these structures is given in Table 1, together with the data ranges used in each case and the dimensions (Δx, Δy, Δz) of each voxel within the unit cell in direct space (used in the calculation of electron density). All structure solution calculations were carried out in space group $P1$, as is common practice in standard CF calculations.

For each test structure, 50 independent calculations were carried out starting from different sets of random initial phases. The progress of the structure solution calculations is monitored by plotting the R-factor [defined here as $R = (\sum_h||F_{exp}(h)| - |G_n(h)||)/(\sum_h|F_{exp}(h)|)$] versus iteration number, and assessing the convergence of the R-factor. After obtaining satisfactory structure solutions (in space group $P1$), relevant origin shifts for the actual space group were carried out using the method described previously by Palatinus and Chapuis.[17] An average electron density map was then determined by averaging the electron density maps for all correct solutions obtained (from the 50 independent calculations). The phase of each structure factor was then calculated from the average electron density map, and the phase information was then input into the *MIFIT* program[23] to plot the final electron density map for comparison to the known crystal structure.

The results from the RBCF structure solution calculations for each of the test structures are shown in Figure 3, in which the final electron density map is compared with the known crystal structure. It is clear that, in each case, the structure solution obtained from the RBCF calculation is in good agreement with the correct crystal structure and would represent a viable starting point for successful structure refinement calculations.

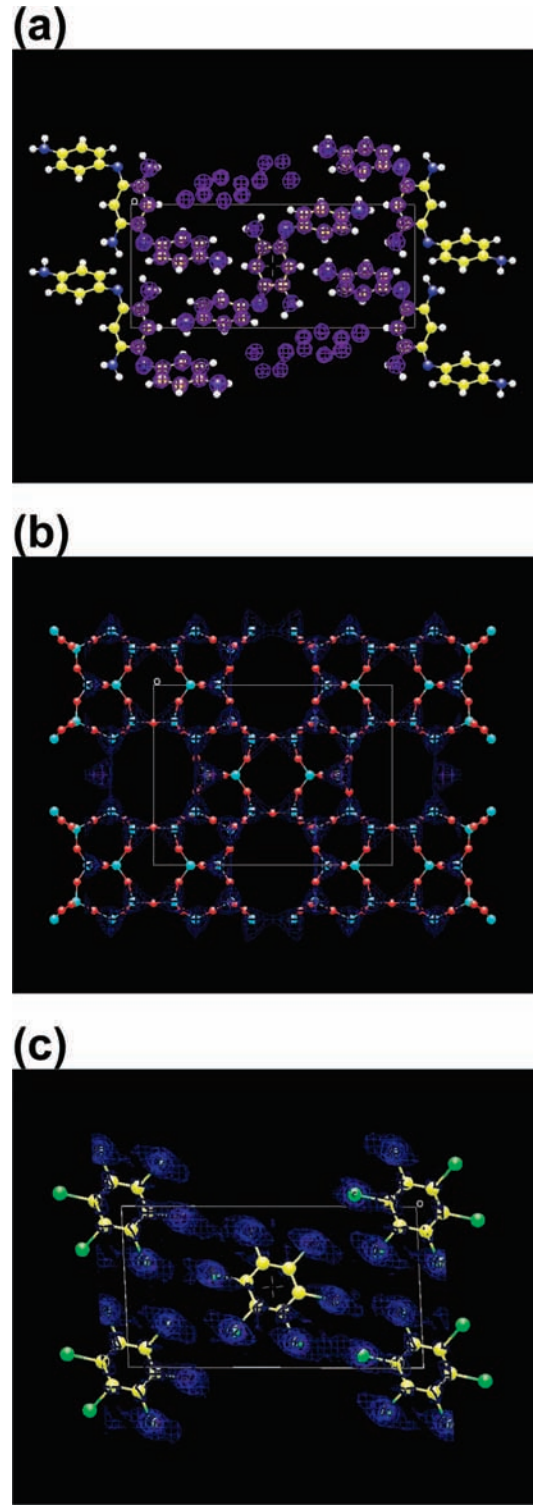

Figure 3. Calculated electron density map (shown in blue for manually selected contour level) for the structure solution obtained in the RBCF calculation superimposed on the known crystal structure for (a) structure **1**, (b) structure **2**, and (c) structure **3**.

Next we consider the success rate of the RBCF calculations. Although RBCF calculations invoke a random element in the sense that the initial phases are generated at random, the calculation thereafter is deterministic and it is not proven that all sets of random initial phases will guarantee convergence of

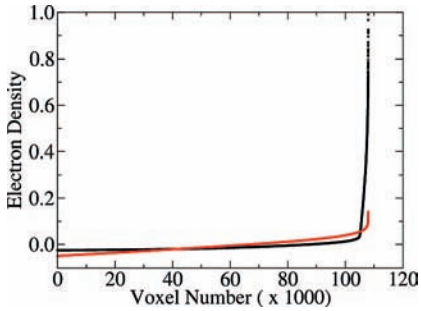

Figure 4. Electron density histograms for the structure solution obtained in a successful RBCF calculation (black) and an unsuccessful RBCF calculation (red). The electron density scale is normalized such that the value of electron density for the voxel of highest electron density is 1.

the calculation on the correct structure solution. To assess the extent to which the success of the calculation depends on the set of random initial phases generated, 50 independent RBCF calculations were carried out from different sets of random initial phases for each of the test structures considered. In all cases, rapid convergence is observed, with the *R*-factor typically decreasing rapidly as a function of iteration number from the start of the calculation (this aspect of the convergence behavior contrasts markedly with standard CF calculations and is discussed in more detail below). However, though convergence on a low *R*-factor value is clearly a *necessary* condition for a successful structure solution calculation, we find that it is not a *sufficient* condition for guaranteeing that the structure solution obtained in the calculation is actually correct. For this purpose, an electron density histogram has been used as a supplementary criterion for assessing the correctness of the structure solution, in which the electron density values (i.e., $\rho_n(r)$, calculated before charge flipping) for all voxels in the unit cell are ranked from lowest electron density (assigned the lowest voxel number) to highest electron density (assigned the highest voxel number), and then displayed as a plot of electron density versus voxel number.[5,13,15] We find that, for all correct solutions obtained for a given structural problem, the electron density histogram takes a characteristic shape and form (see Figure 4) that is essentially the same in all cases, whereas all incorrect structure solutions exhibit an electron density histogram that has substantially different shape. Such comparison provides a strong discrimination between correct and incorrect structure solutions and has been used (in conjunction with the *R*-factor) as the basis for assessing the success rates of the RBCF calculations in this work. On this basis, for the 50 independent calculations carried out for each test structure, we found that 48 calculations resulted in the correct solution for structure **1**, 45 calculations resulted in the correct solution for structure **2**, and all 50 calculations resulted in the correct solution for structure **3**. We note that the success rate is found to be sensitive to the resolution in reciprocal space and direct space, and the quoted success rates refer to the results of calculations employing the resolution values shown in Table 1.

Plots of *R*-factor versus iteration number for the successful structure solution calculations for each test structure are shown in Figure 5. We note that, for a given test structure, the final values of *R*-factor for all the successful calculations span a range of values (rather than converging on the same value), although inspection of the actual electron density maps confirms that they all correspond to the correct structure solutions. The plots of *R*-factor versus iteration number shown in Figure 5 highlight an important difference in the convergence of RBCF calculations

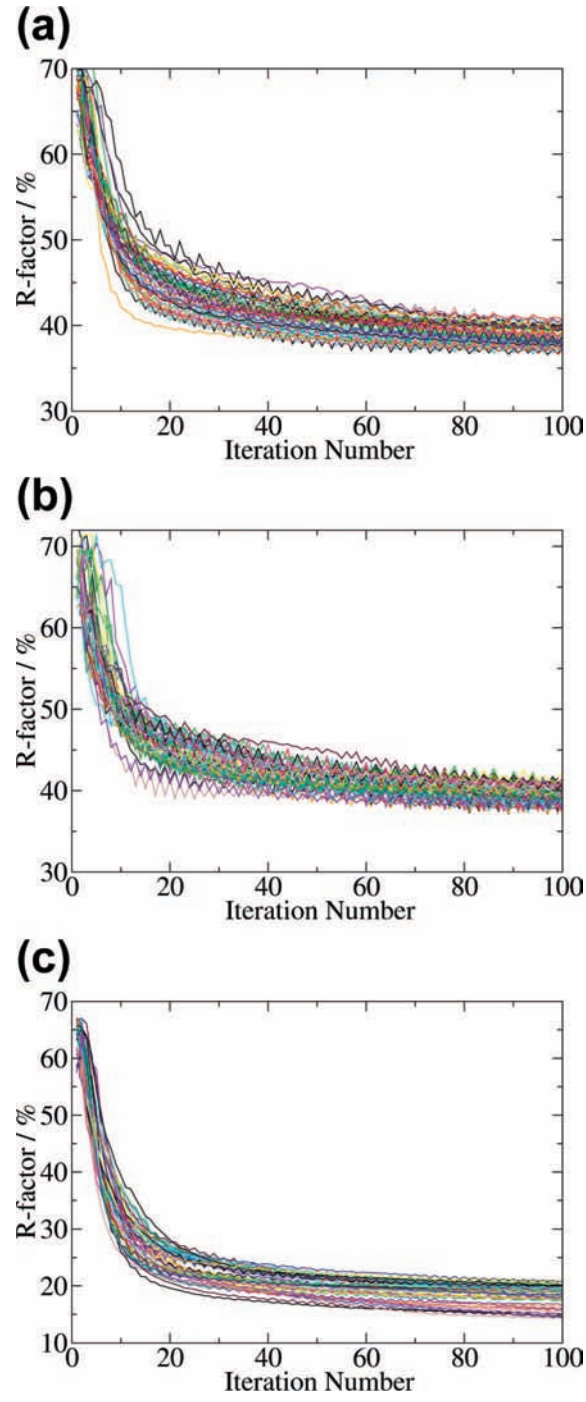

Figure 5. *R*-factor versus number of iterations for the independent structure solution calculations using the RBCF technique for (a) structure **1**, (b) structure **2**, and (c) structure **3**. As discussed in the text, only the results from those calculations leading to the correct structure solution are shown in each case.

in comparison with standard CF calculations. As noted in section 2, plots of *R*-factor versus iteration number for standard CF calculations typically exhibit a long plateau region at high *R*-factor, before the *R*-factor finally drops suddenly as the calculation converges on the correct structure solution. This behavior has been observed repeatedly in different implementations of the standard CF methodology, and the long plateau region can extend in some cases to several thousand or more iterations. In contrast, we find that in virtually all cases, RBCF calculations do not exhibit any plateau region in plots of *R*-factor versus iteration number, with the *R*-factor typically dropping

immediately from the start of the calculation and converging rapidly on the structure solution (see Figure 5). Thus, for RBCF calculations, the rate of decrease of the *R*-factor is typically highest within the earliest iterations of the calculation. This striking contrast in behavior suggests a fundamental difference in the factors that drive the convergence of RBCF calculations in comparison with standard CF calculations, which we are currently exploring in our ongoing research in this field. We envisage that the different convergence behavior observed for RBCF calculations in comparison with standard CF calculations may prove advantageous in certain areas of application.

5. Concluding Remarks

The results reported here demonstrate that the RBCF technique represents a viable and successful strategy for structure solution from X-ray diffraction data. An important feature of the RBCF technique is that it does not require a positive threshold electron density value (δ) to be specified to control the charge-flipping step. In contrast, it is well established that the success of standard CF calculations can depend critically on choosing a suitable value of δ for a given structural problem. We also observe that the convergence behavior of RBCF calculations contrasts markedly with that generally observed for standard CF calculations (with convergence typically progressing rapidly and immediately from the earliest iterations of the calculation, rather than displaying an extended plateau region). This convergence behavior and the fact that the RBCF technique does not use the δ parameter required in standard CF calculations, suggest that the RBCF algorithm may be a promising approach in future applications. We are currently carrying out extensive investigations to further develop the RBCF technique, and to explore in more detail fundamental aspects underlying the optimal application of the RBCF algorithm.

Acknowledgment. We thank Astra Zeneca and Cardiff University for funding. We are grateful to Sir John Meurig Thomas for several stimulating discussions, and to Dr. Li-ling Ooi and Dr. Javier Martí-Rujas for carrying out the single-crystal X-ray diffraction data collection for test structure **1**.

References and Notes

(1) (a) Patterson, A. L. *Phys. Rev.* **1934**, *46*, 372. (b) Patterson, A. L. *Z. Kristallogr.* **1935**, *90*, 517. (c) Hauptman, H. *Angew. Chem., Int. Ed. Engl.* **1986**, *25*, 603. (d) Karle, J. *Angew. Chem., Int. Ed. Engl.* **1986**, *25*, 614. (e) Dunitz, J. D. *X-ray Analysis and the Structures of Organic Molecules*; Verlag Helvetica Chimica Acta: Basel, 1995. (f) Woolfson, M. M. *An Introduction to X-ray Crystallography*, 2nd ed.; Cambridge University Press: Cambridge, U.K., 1997. (g) Sheldrick, G. M. *Acta Crystallogr., Sect. A* **2008**, *64*, 112.

(2) (a) Harris, K. D. M.; Tremayne, M.; Lightfoot, P.; Bruce, P. G. *J. Am. Chem. Soc.* **1994**, *116*, 3543. (b) Harris, K. D. M.; Tremayne, M.; Kariuki, B. M. *Angew. Chem. Int. Ed.* **2001**, *40*, 1626. (c) David, W. I. F., Shankland, K., McCusker, L. B., Baerlocher, C., Eds.; *Structure Determination from Powder Diffraction Data*; OUP/IUCr: 2002. (d) Harris, K. D. M.; Cheung, E. Y. *Chem. Soc. Rev.* **2004**, *33*, 526. (e) David, W. I. F.; Shankland, K. *Acta Crystallogr., Sect. A* **2008**, *64*, 52.

(3) Oszlányi, G.; Sütő, A. *Acta Crystallogr., Sect. A* **2004**, *60*, 134.

(4) Oszlányi, G.; Sütő, A. *Acta Crystallogr., Sect. A* **2005**, *61*, 147.

(5) Baerlocher, C.; Gramm, F.; Massuger, L.; McCusker, L. B.; He, Z. B.; Hovmoller, S.; Zou, X. D. *Science* **2007**, *315*, 1113.

(6) Palatinus, L.; Steurer, W.; Chapuis, G. *J. Appl. Crystallogr.* **2007**, *40*, 456.

(7) Oszlányi, G.; Sütő, A.; Czugler, M.; Párkányi, L. *J. Am. Chem. Soc.* **2006**, *128*, 8392.

(8) Palatinus, L. *Acta Crystallogr., Sect. A* **2004**, *60*, 604.

(9) Piao, S. Y.; Palatinus, L.; Lidin, S. *Inorg. Chem.* **2008**, *47*, 1079.

(10) Lidin, S. in *Turning Points in Solid-State, Materials and Surface Science: A Book in Celebration of the Life and Work of Sir John Meurig Thomas* (Editors: Harris, K. D. M., Edwards, P. P.), Royal Society of Chemistry, Cambridge, 2008, p. 250.

(11) Fleischer, F.; Steurer, W. *Philos. Mag.* **2007**, *87*, 2753.

(12) Wu, J. S.; Leinenweber, K.; Spence, J. C. H. *Nat. Mater.* **2006**, *8*, 647.

(13) Baerlocher, C.; McCusker, L. B.; Palatinus, L. *Z. Kristallogr.* **2007**, *222*, 47.

(14) Oszlányi, G.; Sütő, A. *Acta Crystallogr., Sect. A* **2007**, *63*, 156.

(15) Oszlányi, G.; Sütő, A. *Acta Crystallogr., Sect. A* **2008**, *64*, 123.

(16) Coelho, A. A. *Acta Crystallogr., Sect. A* **2007**, *63*, 400.

(17) Palatinus, L.; Chapuis, G. *J. Appl. Crystallogr.* **2007**, *40*, 786.

(18) Blake, A. J.; Hubberstey, P.; Quinlan, D. J. *Acta Crystallogr. Sect. C* **1996**, *52*, 1774.

(19) Morris, R. E.; Weigel, S. J.; Henson, N. J.; Bull, L. M.; Janicke, M. T.; Chmelka, B. F.; Cheetham, A. K. *J. Am. Chem. Soc.* **1994**, *116*, 11849.

(20) Baharie, E.; Pawley, G. S. *Acta Crystallogr., Sect. A* **1979**, *35*, 233.

(21) Reddy, C. M.; Kirchner, M. T.; Gundakaram, R. C.; Padmanabhan, K. A.; Desiraju, G. R. *Chem. Eur. J.* **2006**, *12*, 2222.

(22) The single-crystal X-ray diffraction data collection for test structure **1** was carried out on an Enraf Nonius Kappa CCD diffractometer at 150 K using Mo Kα radiation ($\lambda = 0.71073$ Å).

(23) Program available from http://www.rigaku.com.

JP801185U